

THE COMPRESSIVE AND SHEAR RESPONSES OF CORRUGATED HIERARCHICAL AND FOAM FILLED SANDWICH STRUCTURES

S. Kazemahvazi^{*} and D. Zenkert^{*}

^{*} Kungliga Tekniska Högskolan, KTH
100 44 Stockholm, Sweden

e-mail: sohrabk@kth.se and danz@kth.se, web page: <http://www.kth.se>

Key words: Corrugated cores, Smart structures, Hierarchical structures, Foam filled cores.

Summary. *The mechanical behaviour of two types of corrugated sandwich cores are investigated experimentally and modelled analytically; (i) Corrugation with monolithic composite elements and (ii) a hierarchical sandwich structure (with sandwich core elements). An additional core design, foam filled corrugation, is investigated experimentally and compared to the aforementioned designs. Results show that the hierarchical structure has significantly higher specific strength than the monolithic and foam filled core designs.*

1 INTRODUCTION

Sandwich structures with cellular cores have proven superior weight specific stiffness and strength properties compared to its monolithic counterpart. Polymer foams and hexagonal honeycomb structures are commonly used as core materials. During the past years, many core designs with improved quasi-static and dynamic performance have been proposed. These comprise aluminium foams and various metallic core topologies such as truss- and plate-like configurations [1]. Numerous metallic truss configurations have been proposed with competitive quasi-static properties [2] and dynamic properties [3]. The metallic plate configurations include various honeycomb cores (square, hexagonal, triangular) [4] and prismatic cores (diamond lattice and corrugations) [5]. Further, Kooistra *et al* [6] have analysed the behaviour of corrugated hierarchical metal sandwich panel concepts. Their results show that the second order structure has significantly higher weight specific strength performance than its first order counterpart while the weight specific stiffness tend to decrease with increasing structural hierarchy.

Using fibre composite materials to manufacture the aforementioned core topologies increases the design space additionally and consequently further optimisation of the structure can be done; this due to the anisotropic nature of the composite materials. Composite corrugation cores introduce other failure modes compared to that of metallic structures. As an example, material rupture occurs instead of plastic buckling when the core members are subjected to large bending deformations. In addition to the differences in failure modes, it is also necessary to know in which lamina failure occurs. In order to predict such failure

mechanisms, knowledge of the stress distribution over the entire core members is necessary.

Recently, Kazemahvazi and Zenkert [7] developed models suitable for predicting stiffness and strength of all composite corrugated sandwich cores. The strength model is based on the stress distribution prediction over each core member when the sandwich core is subjected to a shear or compressive load condition. The strength model also accounts for initial imperfections that may arise during the manufacturing process.

Within this work, the previously mentioned model is extended to account for shear deformations in addition to bending and stretching deformations. The model is used to predict the compressive and shear strength of an all composite hierarchical sandwich structure, see figure 1c. Further, an experimental programme is conducted in order to compare the compressive and shear response of three different all composite corrugated core designs. The different core designs are: (i) A corrugation where each core element is a monolithic composite shell, see figure 1(a), (ii) a foam filled version of (i), see figure 1(b), and (iii) each core element is a sandwich plate (hierarchical sandwich structure), see figure 1(c).

The outline of the paper is as follows. First manufacturing methods and the experimental programme are described. Second, we briefly review the analytical model for strength prediction of corrugated monolithic cores. A strength model for the hierarchical sandwich structure is then described and failure mechanism maps are used to discuss appropriate core designs. Finally, we compare the properties of the three corrugation cores and summarise the experimental findings.

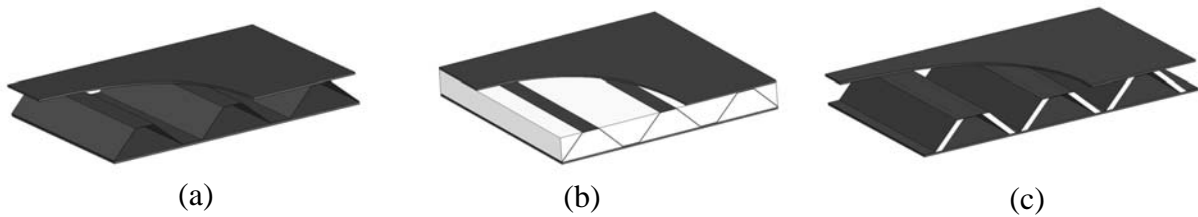


Figure 1: Three different sandwich cores. (a) Monolithic composite core elements, (b) foam filled composite corrugation and (c) composite sandwich core elements (hierarchical sandwich structure).

2 MANUFACTURING ROUTES AND EXPERIMENTAL PROTOCOL

The monolithic corrugated core was manufactured using a machined aluminium mould. Prepreg laminae were stacked to obtain the desired thickness and the laminate was cured for 1 hour in 120°C under vacuum pressure, see figure 2a. The hierarchical corrugation core was manufactured in the same way as the monolithic corrugation with the addition of PMI foam (Rohacell) in the core members, see figure 2b. The foam filled corrugated cores were manufactured as shown in figure 2c. The foam was cut into trapezoid shapes and bonded to a pre-cured monolithic corrugation using structural adhesives. A summary of the tested corrugation configurations is found in table 1. At least two specimens of each corrugation configuration were tested and all results are presented as mean values of the conducted experiments.

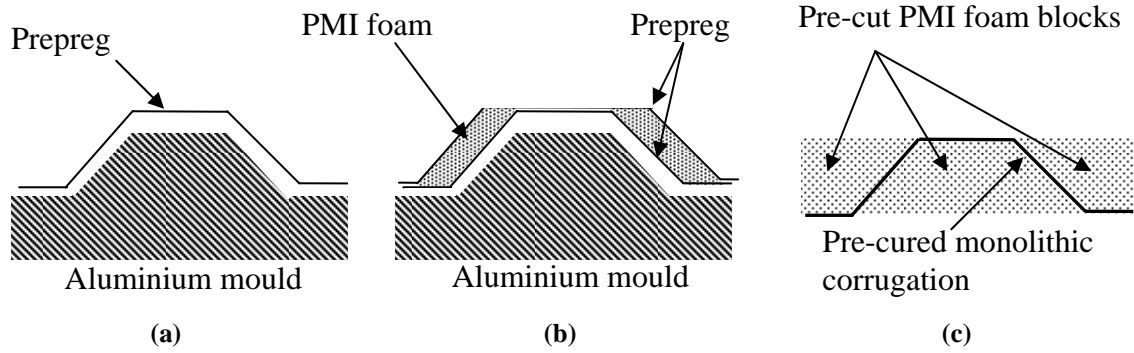


Figure 2: Manufacturing route of (a) monolithic corrugation, (b) hierarchical corrugation structures and (c) foam filled corrugation structure.

	Core member length, l_1	Web/face thickness, t, t_f	Core member core thickness, t_{cweb}	Core member core/filling density, ρ_{cweb}	Core density ρ_c
Monolithic 1	35.16 mm	0.4 mm	--	--	34 kgm ⁻³
Monolithic 2	35.16 mm	1.2 mm	--	--	100 kgm ⁻³
Hierarchical 1	35.16 mm	0.2 mm	5.1 mm	32 kgm ⁻³	42 kgm ⁻³
Hierarchical 2	35.16 mm	0.2 mm	5.1 mm	110 kgm ⁻³	58 kgm ⁻³
Foam filled 1	35.16 mm	0.4 mm	--	32 kgm ⁻³	65 kgm ⁻³
Foam filled 2	35.16 mm	0.4 mm	--	51 kgm ⁻³	85 kgm ⁻³

Table 1: Corrugation configurations tested in the experimental programme. The geometrical variables are shown in figure 4.

2.1 Constitutive material

The corrugations were made of unidirectional carbon fibre SE-84LV prepreg system supplied by Gurit. All corrugations were made using unidirectional laminates with the fibre direction along the corrugation. Material properties for a unidirectional lamina are presented in table 2.

E_1 [GPa]	140
E_2 [GPa]	7.45
G_{12} [GPa]	3.85
$\hat{\sigma}_{1t}$ [MPa]	1950
$\hat{\sigma}_{1c}$ [MPa]	858
$\hat{\sigma}_{2t}$ [MPa]	26.6

Table 2: Material properties of unidirectional SE-84LV carbon fibre prepreg. E is the Young's modulus, G the shear modulus and $\hat{\sigma}$ the ultimate strength. The notations 1 and 2 refer to the direction of the load where 1 is along the fibres and 2 is transverse the fibres. The notations t and c refers to tensile or compressive loading.

2.2 Test method

Single-block shear tests were conducted according to ASTM C273-00. Two unit cells of the corrugation were bonded to rigid steel blocks and tensile loading was applied at the ends of the rigid plates, see figure 3(a). Deflections were measured using extensometers and digital calipers. Compression tests were conducted on a unit cell of the corrugation mounted between two stiff steel plates, see figure 3(b). All experiments were conducted in a screw-driven 30kN test machine at a quasi-static strain rate.

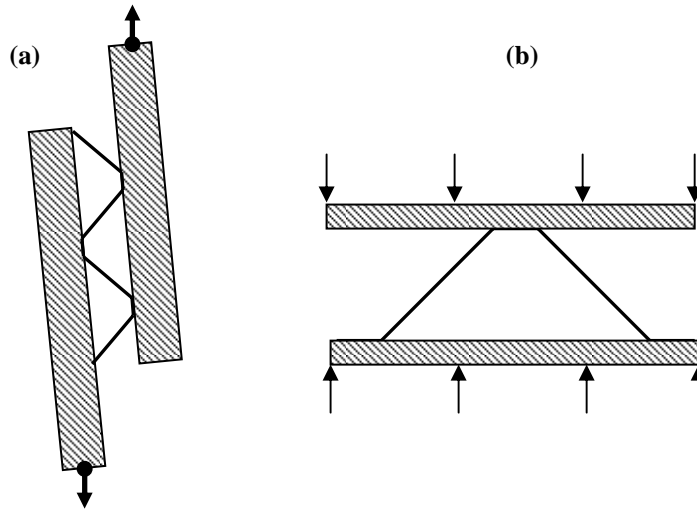


Figure 3: (a) Testing of the core shear properties and (b) testing of the out-of-plane properties of the core.

3 BRIEF SUMMARY OF ANALYTICAL MODELS

3.1 Compressive and shear response of a monolithic core

Consider a unit cell of a corrugated core with geometrical quantities as specified in figure 4. Assume that each core member is built-in to the face sheets so that the ends of the members have clamped boundary conditions. The equivalent shear and compressive modulus of the core is given by equation 1 and equation 2, respectively [7]. D_{11} is the bending stiffness of the core member, S_1 is the shear stiffness and A_{11} is the extensional stiffness component. For isotropic materials A_{11} reduces to Et , where E is the Young's modulus of the material and t is the thickness.

$$G_{xz} = \frac{\tau_{xz}}{\gamma_{xz}} = \frac{\sin \omega}{(l_1 \cos \omega + l_2)} \left[A_{11} \cos^2 \omega + \frac{\sin^2 \omega}{\frac{l_1^2}{12D_{11}} + \frac{1}{S_1}} \right] \quad (1)$$

$$E_{zz} = \frac{\sigma_{zz}}{\varepsilon_{zz}} = \frac{\sin \omega}{(l_1 \cos \omega + l_2)} \left[A_{11} \sin^2 \omega + \frac{\cos^2 \omega}{\frac{l_1^2}{12D_{11}} + \frac{1}{S_1}} \right] \quad (2)$$

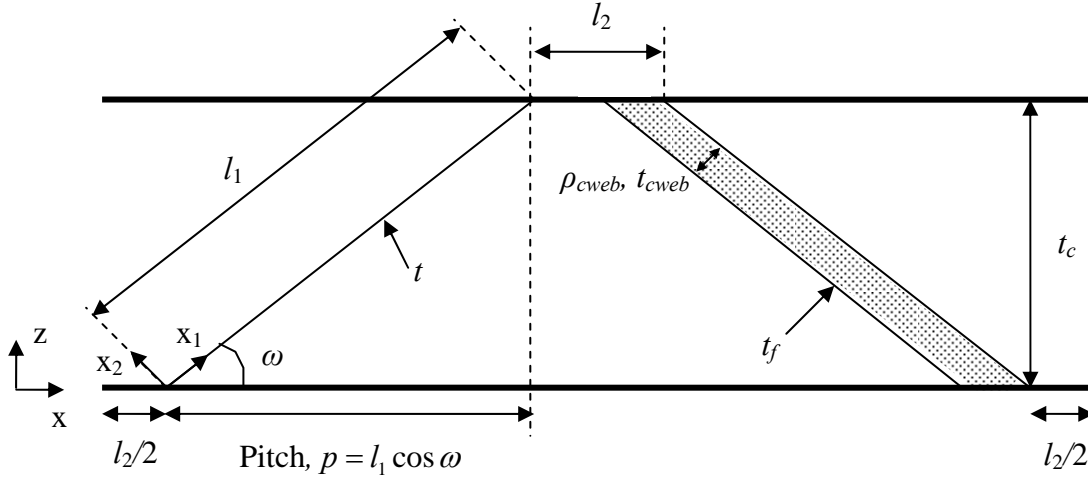


Figure 4: Unit cell of a corrugated core. The left core member shows a monolithic version and the right core member shows a sandwich version.

Consider the compression loaded part of a unit cell as described in figure 5. Due to the clamped end condition of the core members they will undergo both stretching and bending deformation. Due to the presence of bending deformations, the in-plane stretching force (N_1) causes additional bending deformation that must be taken into account in order to capture elastic instability phenomena. Further, each core member is assumed to have an initial imperfection in the shape of the first buckling mode of a clamped strut.

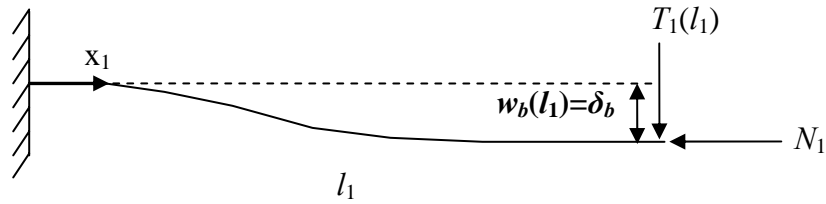


Figure 5: Beam problem that corresponds to a unit deformation of a core web.

For slender monolithic core members shear deformations are assumed to be negligible. The in-plane stretching force (N_1) is assumed to be constant over the entire core member and the transverse force T_1 is chosen so that the bending deformation at the end of the beam equals a

unit deflection δ_b . The ordinary differential equation that describes the deformation of the core member is solved analytically and a closed form solution for the bending deformation $w_b(x_1)$ is obtained. Consequently, the bending moment $M(x_1)$ and the transverse force $T(x_1)$ distributions are obtained. A simple strength model can now be employed based on the strength of the material. Failure of the core is assumed when, (i) the applied load is within 2 percent of the critical buckling load or (ii) the compressive stresses exceed the compressive strength of the laminate or (iii) the tensile stresses exceed the tensile strength of the laminate.

3.2 Compressive and shear response of a core with sandwich core members

The model described in section 3.1 is now extended to account for shear deformation in addition to the bending and stretching deformation. The initial imperfections of the core members are however neglected in this analysis. The same solution method, as for the model described in section 3.1, is used to obtain the closed form solution of the deformation of a sandwich core member. Again, the bending moments $M(x_1)$ and the transverse forces $T(x_1)$ are obtained explicitly. A strength model based on five competing failure modes is now employed. The different failure modes are shown schematically in figure 6 and the failure criteria are described in subsequent sections.

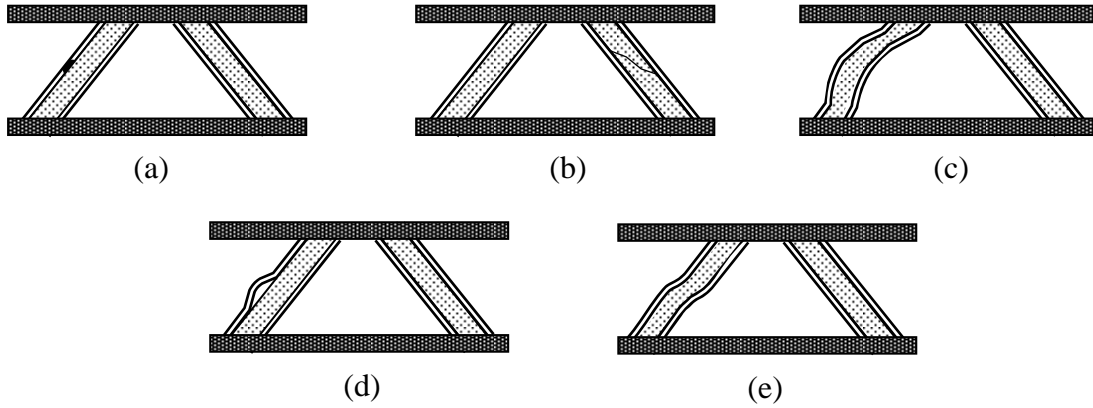


Figure 6: Failure modes of composite corrugation with sandwich core members. (a) Face fracture, (b) core shear failure, (c) general buckling, (d) local buckling/wrinkling and (e) shear buckling.

3.2.1 Face fracture

Face fracture (figure 6a) is assumed to occur when the compressive stress in a face reaches the ultimate compressive strength of the material, $\hat{\sigma}_f$. This is given by,

$$\sigma_f = \frac{M_1^{\max} d}{2D_{11}} E_f + \frac{N_1}{t_f} \geq \hat{\sigma}_f \quad (3)$$

where t_f is the core member face thickness, t_{cweb} the core member core thickness, $d = t_{cweb} + t_f$ and E_f the modulus of the core member face sheet.

3.2.2 Core shear failure

Shear failure of the core elements (figure 6b) is assumed to occur when the shear stress in the core reaches the ultimate shear strength of the core material, $\hat{\tau}_{12}$. This is given by,

$$\tau_{12} = \frac{T_1^{\max}}{d} \geq \hat{\tau}_{12} \quad (4)$$

3.2.3 General Buckling

The mode I symmetrical buckling load (figure 6c) of a clamped sandwich column is given by equation 5 [8]. General buckling is thus assumed to occur when the compressive force acting on the core member reaches this critical value.

$$N \geq N_{cr} = \frac{\frac{4\pi^2 D_{11}}{l_1^2}}{1 + \frac{4\pi^2 D_{11}}{l_1^2 S_1}} \quad (5)$$

3.2.4 Face wrinkling/local buckling

Hoff's method [9] has been used as a failure criterion for local buckling, see figure 6d. Local buckling is assumed to occur when the compressive stress in a face reaches the critical local buckling stress as specified in equation 6.

$$\sigma_f \geq \sigma_{cr}^{Localbuckling} = 0.5\sqrt[3]{E_f E_c G_c} \quad (6)$$

where E_c is the modulus and G_c the shear modulus of the core material.

3.2.5 Shear buckling

The shear buckling of a core member (figure 6e) is set by its shear stiffness, S_1 , as discussed in [8]. Shear buckling is thus assumed to occur when,

$$N_1 \geq S_1. \quad (7)$$

3.2.6 Failure mechanisms

In order to validate the analytical model for a range of configurations and failure modes, failure mechanism maps were created. Using these maps different core member configurations with different failure modes could be chosen for the experimental programme. Figure 7 shows a failure mechanism map for a 45-degree corrugation with sandwich core members loaded in out-of-plane compression or shear. The face thickness and the length of the core members are fixed while the core density (ρ_{cweb}) and core thickness (t_{cweb}) of the core

members are altered. For a core thickness of 5 mm three different failure modes can occur depending on the core density. For low core density, $<45 \text{ kgm}^{-3}$, the core members are predicted to fail in general buckling. For intermediate core densities, 45 kgm^{-3} - 170 kgm^{-3} , the core member is predicted to fail by local buckling and at high core densities $>170 \text{ kgm}^{-3}$ the core member is predicted to fail by face fracture.

Figure 8 shows two different corrugation configurations subjected to out-of-plane compressive loading. One is manufactured with a low density foam (figure 8a), Hierarchical 1, and another with an intermediate density foam (figure 8b), Hierarchical 2. Photographs clearly show that the core configuration with low density foam fails in a general buckling mode while the one with intermediate density foam fails through local buckling of the faces.

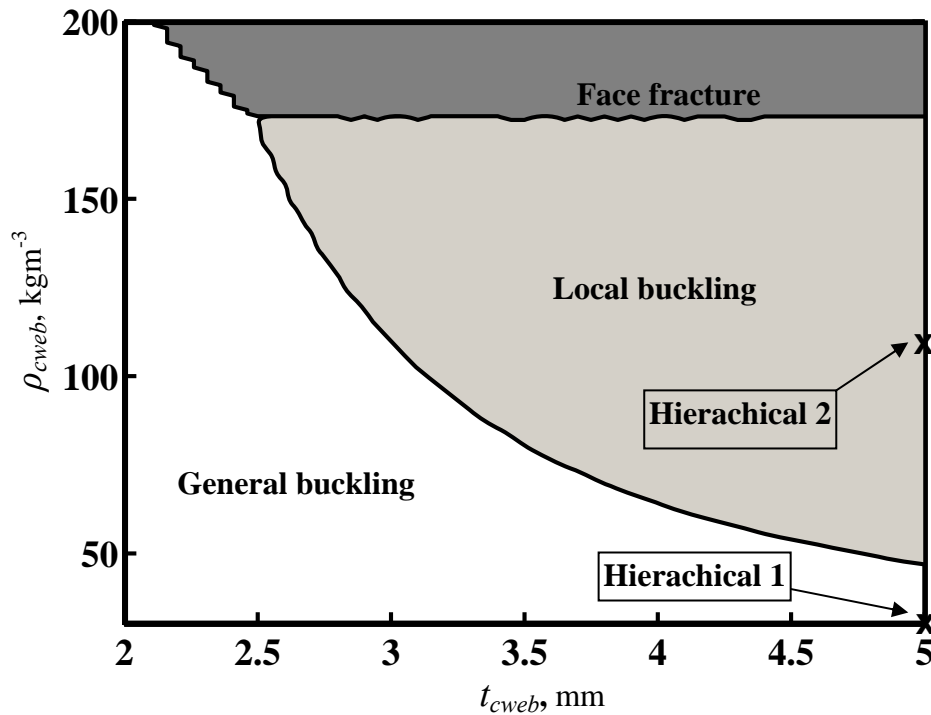


Figure 7: Failure mechanism map for a 45-degree corrugation with sandwich core members. The same failure mechanism map is found for both compression and shear loading in the case of a 45-degree corrugation.
 $t_f = 0.2 \text{ mm}$ and $l_1 = 35.16 \text{ mm}$.

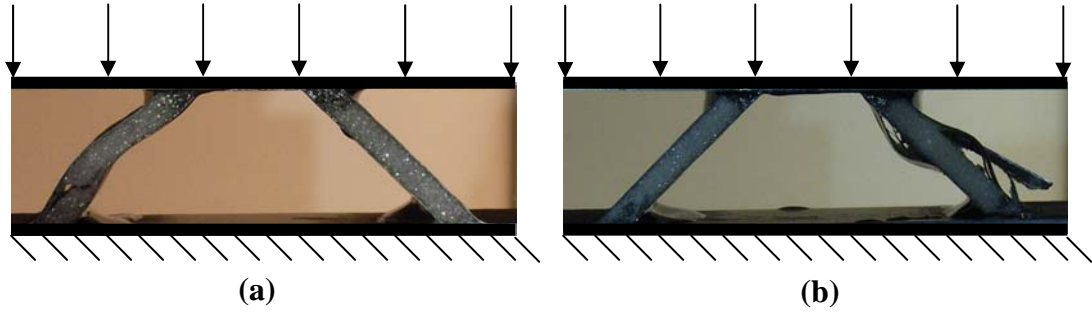


Figure 8: Photographs taken during out-of-plane compression experiment. (a) Hierarchical 1 configuration and (b) Hierarchical 2 configuration.

4 COMPARISON OF CORE DESIGNS

4.1 The out-of-plane compression response

Figure 9 shows a summary of the out-of-plane compressive strength of the three core designs. The core strength, which is normalised with the compressive strength of the material, is plotted as function of the total core density.

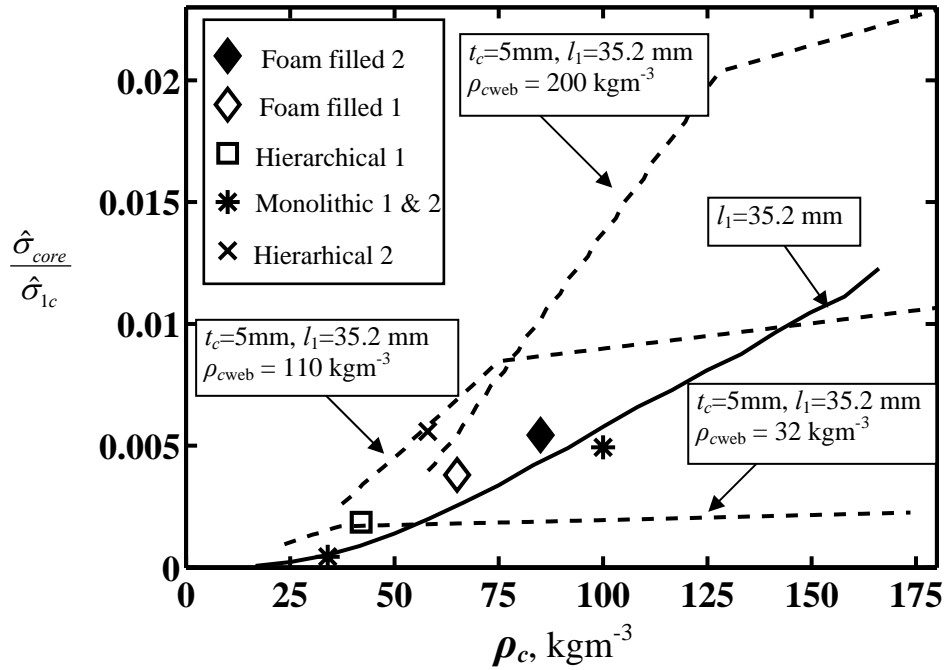


Figure 9: Out-of-plane compressive strength for the three different core designs. Solid line is the analytical model for a monolithic core with an initial imperfection of $0.7t$, dashed lines are the analytical models for the hierarchical structures with various core densities and the free points are mean values of the experimental results.

The strength of the hierarchical structures (dashed lines) is plotted for three different core member core densities as specified in the figure. The core member length is kept constant while the thicknesses of the faces/laminates have been altered. The sandwich core members have face thicknesses ranging from 0.1 mm to 1 mm and the monolithic core thicknesses range from 0.2 mm to 2 mm. Experimental results are included as free points.

4.1.1 Comparison of cores at low densities; $25\text{kgm}^{-3} - 50\text{kgm}^{-3}$

At low core densities the hierarchical structure with a core member core density $\rho_{cweb} = 32\text{kgm}^{-3}$ is 5 times stronger than the monolithic version. At a core density of 32kgm^{-3} the failure mode shifts from local buckling to general buckling which results in a decrease of the slope angle. As the core density increases the monolithic core gains better performance than the $\rho_{cweb} = 32\text{kgm}^{-3}$ hierarchical structure. Recall that the hierarchical structures presented here are not optimised and by alternation of design variables such as core thickness, core density, face thickness etc. potentially better performance can be achieved.

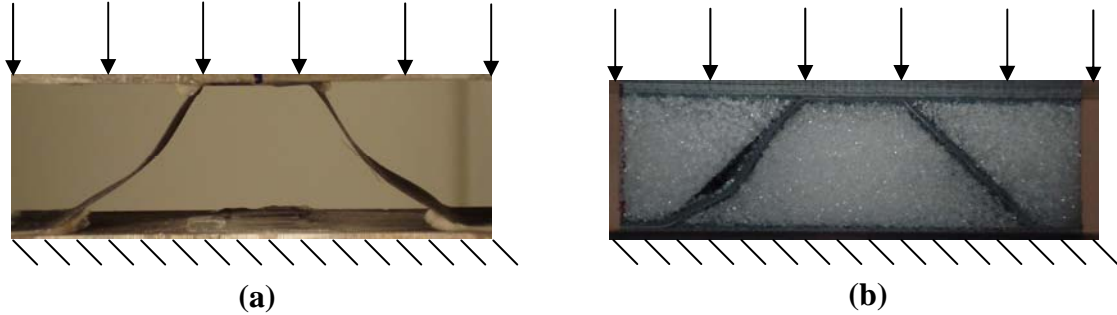


Figure 10: Out-of-plane compression experiment for (a) monolithic core and (b) foam filled core.

4.1.2 Comparison of cores at intermediate and high densities; $50\text{kgm}^{-3} - 175\text{kgm}^{-3}$

As the total core density increases the $\rho_{cweb} = 110\text{kgm}^{-3}$ hierarchical structure outperforms both the monolithic core and the $\rho_{cweb} = 32\text{kgm}^{-3}$ hierarchical core. At a total density of 75kgm^{-3} this core has approximately three times higher strength than the monolithic version.

At a total core density of approximately 75kgm^{-3} the $\rho_{cweb} = 110\text{kgm}^{-3}$ and $\rho_{cweb} = 200\text{kgm}^{-3}$ hierarchical structure are equally strong. The decrease of the slope angle, seen at this point, is due to a failure mode shift from local buckling to general buckling. At the highest core densities studied here the $\rho_{cweb} = 200\text{kgm}^{-3}$ hierarchical structure outperforms the other core designs. This core fails through face fracture at low densities and at a density of 126kgm^{-3} the failure mode shifts to shear buckling which results in a decrease of the slope angle. At a density of 169kgm^{-3} , the failure mode shifts to general buckling. This failure mode shift does, however, not result in a change of slope angle.

Since the predominant failure mode of the monolithic cores at low densities are elastic buckling (see figure 10a), the inclusion of an elastic support increases the strength of the core, this is seen for the experimental results of the foam filled core. The improvement of the performance is, however, not as significant as for the hierarchical structure. This, since the foam filled cores add significantly more weight to the structure compared to the hierarchical

version. Figure 10b shows a foam filled core with a foam density of 32 kgm^{-3} loaded in out of plane compression. The failure mode is a combination of buckling on elastic foundation and compressive failure of the foam.

4.2 The shear response

Same observations are made for the shear response of the structure as for the compressive response, see figure 11. The experimental results for the Hierarchical 2 structure is however considerably lower than the analytical prediction. This is due to an unexpected peel of failure mode of the tensile loaded core member, see figure 12. The foam filled 2 structure failed at the interface between the shear blocks and the core. The true strength of this structure is thus expected to be higher.

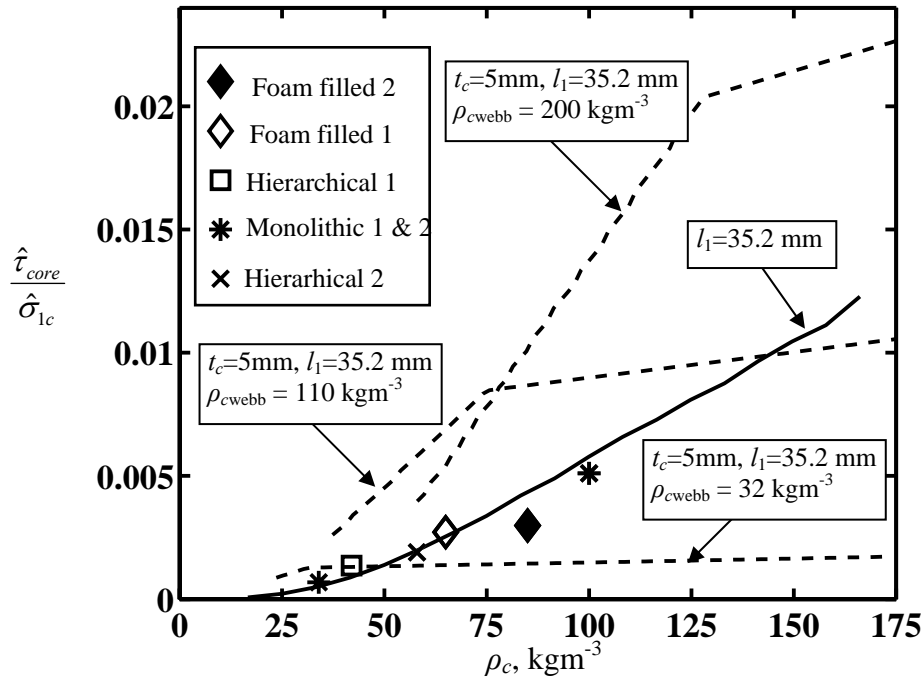


Figure 11: Shear strength for the three different core designs. Solid line is the analytical model for a monolithic core with an initial imperfection of $0.7t$, dashed lines are the analytical models for the hierarchical structures with various core densities and the free points are mean values of the experimental results.

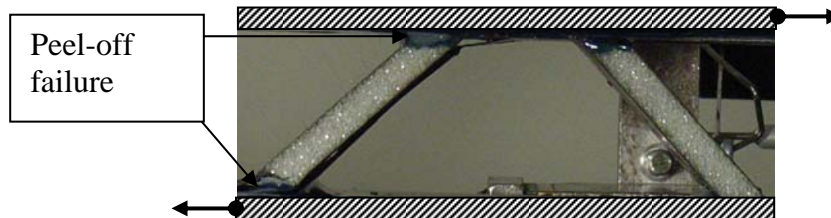


Figure 12: Shear testing of hierarchical 2 structure. The tensile loaded core member fails due to high peel-off stresses at the boundaries.

5 CONCLUDING REMARKS

The compressive and shear performance of three different all-composite core designs has been investigated: (i) A corrugation where each core element is a monolithic composite shell, (ii) a foam filled version of (i) and (iii) each core element is a sandwich plate (hierarchical sandwich structure). Previously developed analytical model for composite corrugations has been extended in order to predict the shear and compressive strength of a corrugated hierarchical sandwich structure. The model shows good agreement with the experimental strength results as well as the obtained failure modes.

The hierarchical structures tested in this study have at least three times higher weight specific strength compared to the monolithic version. Due to the large number of design variables, a fully optimised hierarchical structure potentially has even higher specific strength.

At low core densities, foam filled corrugation cores have higher specific strength compared to the monolithic version but lower strength compared to the hierarchical structure.

ACKNOWLEDGEMENTS

The financial support for this investigation has been provided by The Office of Naval Research (ONR) through programme officer Dr. Yapa D.S. Rajapakse (Grant No. N00014-07-1-0344). Authors would like to express their gratitude to Daniel Tanner for his help during the experimental programme.

REFERENCES

- [1] Wadley HNG., "Multifunctional periodic cellular metals", *Philos T R Soc A*, 2006, 364, 31-68.
- [2] Kooistra GW, Deshpande VS, Wadley HNG., "Compressive behavior of age hardenable tetrahedral lattice truss structures made from aluminium", *Acta Mater.*, 2004, 52, 4229-4237.
- [3] McShane GJ, Radford DD, Deshpande VS, Fleck NA., "The response of clamped sandwich plates with lattice cores subjected to shock loading", *European Journal of Mechanics - A/Solids*, 2006; 25, 2, 215-229.
- [4] Côté F, Deshpande VS, Fleck NA, AG Evans, "The out-of-plane compressive behaviour of metallic honeycombs", *Material Science and Engineering A*, 2004, 380, 272-280.
- [5] Côté F, Deshpande VS, Fleck NA, AG Evans, "The compressive and shear responses of corrugated and diamond lattice materials", *Int J Solid Struct.*, 2006, 43, 6220-6242.
- [6] Kooistra GW, Deshpande VS, Wadley HNG, "Hierarchical corrugated core sandwich panel concepts", *Journal of Applied Mechanics*, 2007, 74, 259-268.
- [7] Kazemahvazi S, Zenkert D., "Compressive and shear response of corrugated all-composite sandwich cores", Submitted for publication 2008.
- [8] Zenkert D. *An introduction to sandwich construction*, Engineering Materials Advisory Service, 1995, Sheffield, UK.
- [9] Hoff N.J. and Mautner S.E., "Buckling of sandwich type panels", *Journal of the Aeronautical Sciences*, 1945, 12, 285-297.